A Change in Liver Metabolism but Not in Brown Adipose Tissue Thermogenesis Is an Early Event in Ovariectomy-Induced Obesity in Rats

Mariana Nigro, Anderson T. Santos, Clarissa S. Barthem, Ruy A. N. Louzada, Rodrigo S. Fortunato, Luisa A. Ketzer, Denise P. Carvalho, and Leopoldo de Meis

Laboratório de Bioenergética (M.N., A.T.S., C.S.B., L.A.K., L.d.M.), Instituto de Bioquímica Médica, Laboratório de Radiobiologia Molecular (R.S.F.) and Laboratório de Fisiologia Endócrina Doris Rosenthal (R.A.N.L., D.P.C.), Instituto de Biofísica Carlos Chagas Filho, Universidade Federal do Rio de Janeiro, Rio de Janeiro 21941–902, Brazil

Menopause is associated with increased visceral adiposity and disrupted glucose homeostasis, but the underlying molecular mechanisms related to these metabolic changes are still elusive. Brown adipose tissue (BAT) plays a key role in energy expenditure that may be regulated by sexual steroids, and alterations in glucose homeostasis could precede increased weight gain after ovariectomy. Thus, the aim of this work was to evaluate the metabolic pathways in both the BAT and the liver that may be disrupted early after ovariectomy. Ovariectomized (OVX) rats had increased food efficiency as early as 12 days after ovariectomy, which could not be explained by differences in feces content. Analysis of isolated BAT mitochondria function revealed no differences in citrate synthase activity, uncoupling protein 1 expression, oxygen consumption, ATP synthesis, or heat production in OVX rats. The addition of GDP and BSA to inhibit uncoupling protein 1 decreased oxygen consumption in BAT mitochondria equally in both groups. Liver analysis revealed increased triglyceride content accompanied by decreased levels of phosphorylated AMP-activated protein kinase and phosphorylated acetyl-CoA carboxylase in OVX animals. The elevated expression of gluconeogenic enzymes in OVX and OVX + estradiol rats was not associated with alterations in glucose tolerance test or in serum insulin but was coincident with higher glucose disposal during the pyruvate tolerance test. Although estradiol treatment prevented the ovariectomy-induced increase in body weight and hepatic triglyceride and cholesterol accumulation, it was not able to prevent increased gluconeogenesis. In conclusion, the disrupted liver glucose homeostasis after ovariectomy is neither caused by estradiol deficiency nor is related to increased body mass. **(*Endocrinology* 155: 2881–2891, 2014)**

Estrogen deficiency is accompanied by increases in body weight associated with higher visceral adiposity. Obesity-related metabolic complications, such as insulin resistance, type 2 diabetes, and cardiovascular diseases, are related to this condition (1, 2) and are observed in postmenopausal women and in animal models of castration or estradiol (E2) signaling deficiency. Accordingly, ovariectomized (OVX) mice (3, 4), aromatase knockout (ArKO) mice (5), and estrogen receptor (ER)-α knockout mice (6) all develop obesity.

Although estradiol deficiency slightly increases food intake (7–9), hyperphagia does not seem to be the primary cause of obesity in animals with disrupted estradiol signaling. Interestingly, OVX animals pair fed to OVX that

ISSN Print 0013-7227 ISSN Online 1945-7170
Printed in U.S.A.

Received April 25, 2013. Accepted May 29, 2014.
First Published Online June 10, 2014

Abbreviations: ACC, acetyl-CoA carboxylase; AMPK, AMP-activated protein kinase; ArKO, aromatase knockout; BAT, brown adipose tissue; b.w., body weight; E2, estradiol; ER, estradiol receptor; G6Pase, glucose 6-phosphatase; HDL, high-density lipoprotein; HMG-CoA, 3-hydroxy-3-methylglutaryl coenzyme A; LDL, low-density lipoprotein; LKB1, liver kinase B1; OVX, ovariectomized; p, phosphorylated; PEPCK, phosphoenolpyruvate carboxykinase; PGC-1α, peroxisome proliferator-activated receptor γ coactivator 1-alpha; SREBP1c, sterol regulatory element-binding protein 1c; TG, triglyceride; TRAF2, TNF receptor-associated factor 2; UCP1, uncoupling protein 1; VLDL, very low-density lipoprotein.

received E2 (OVX + E2) gain more weight than the group receiving E2 (3), suggesting that alterations in energy expenditure may play a role in the obese phenotype of OVX animals. In fact, recent reports have shown decreased energy expenditure not only after ovariectomy (1, 10) but also when ERα is silenced in the ventromedial nucleus of the hypothalamus, a key center of energy homeostasis (8). However, the mechanisms underlying these changes in energy expenditure are not well understood and may be a consequence rather than a cause of the weight gain.

Brown adipose tissue (BAT) plays a key role in thermogenesis in small rodents and newborn humans. The thermogenic ability of BAT is attributed to the high abundance of mitochondria found in this tissue and the unique presence of uncoupling protein 1 (UCP1) in the mitochondrial inner membrane. When activated, UCP1 uncouples the proton electrochemical gradient from ATP synthesis (11, 12). Recent data indicate that adult humans also have UCP1-positive fat depots, and these results have increased the interest in the contribution of BAT to body weight regulation in humans (13, 14). Previous studies have shown gender dimorphism in the thermogenic capacity of BAT (15, 16), such as differences in the levels of adrenergic receptors, the size of mitochondria and UCP1 content (17). Nadal-Casellas et al (18) reported an increase in the amount of mitochondrial DNA but a decrease in oxidative capacity in BAT at 5 weeks after ovariectomy. Taken together, these data raise the question of whether decreased BAT activity could be an early event linked to the increased weight gain that occurs after ovariectomy.

Concomitant with body weight gain, postmenopausal women also display increased incidence of hepatic steatosis (19) and disrupted glucose homeostasis (2, 20). E2 signaling in the liver is important in the prevention of diabetes mellitus and hepatic steatosis (21, 22) because this steroid hormone suppresses the expression of enzymes involved in lipogenesis in mice fed a high-fat diet (23). Animals devoid of aromatase activity (ArKO) display hepatic steatosis associated with a decrease in the expression and activity of fatty acid β-oxidation enzymes in the liver (24). Further evidence indicates that E2 down-regulates hepatic glucose production (21, 25–27), but it is not known whether increased gluconeogenesis is secondary to the accumulation of fat in the liver and whether it precedes insulin resistance. Moreover, Liu et al (28) recently reported an increased endogenous glucose production after E2 administration in the ventromedial hypothalamic nucleus of OVX rats. Thus, although hepatic glucose production is regulated by a balance between insulin and counterregulatory hormones (29), the E2 effect on gluconeogenesis is not fully understood and requires further investigation.

Thus, the goal of this work was to evaluate whether impaired BAT thermogenic activity or changes in liver metabolic parameters are involved in the early events related to increased body weight gain in OVX rats. The result was that, early after ovariectomy, we observed hepatic metabolic changes that led to an increased glucose production that was not prevented by estradiol treatment and triacylglycerol accumulation that was completely prevented by estradiol.

Materials and Methods

Experimental groups

Female Wistar rats weighing approximately 200 g (2 mo old) were maintained at 22°C in a 12-hour light, 12-hour darkness cycle. Food and water were available ad libitum. The rats were divided into three groups: sham-operated (SHAM), ovariectomized (OVX), and ovariectomized treated with 17β-estradiol [7 μg/kg body weight (b.w.)]. Animals were individually housed, and food intake, feces amount, and body weight gain were monitored. Twelve or 20 days after ovariectomy, the rats fasted overnight (during the light cycle) and were euthanized by decapitation. Blood was collected from the trunk, and serum was obtained by centrifugation of the blood at 1500 $\times$ *g* for 20 minutes. The Institutional Committee for Use of Animals in Research approved the study (number IBQM062).

Glucose, insulin, and pyruvate tolerance tests

These tests were performed at 12 or 21 days after ovariectomy. To test for glucose tolerance, rats were fasted overnight, and glucose levels were measured before and after glucose injection (1.75 g/kg b.w., administered ip) using commercially available glucose test strips and a glucometer (Accu-Chek Active). The blood glucose concentration was measured over a period of 90 minutes. The same procedure was used for the pyruvate and insulin tolerance tests, but instead of glucose, sodium pyruvate (2 g/kg b.w.) and insulin (0.75 U/ kg b.w.) were injected ip.

Serum analyses

Triglycerides, cholesterol, and high-density lipoprotein (HDL) were determined using commercial kits (Bioclin); very low-density lipoprotein (VLDL) and low-density lipoprotein (LDL) were calculated according to the Friedewald equation. Serum insulin was determined by an ELISA (EZRMI-13K; Millipore). Estradiol and progesterone were determined by an electrochemiluminescence immunoassay (Modular Analytic E170; Roche Diagnostics). FSH and LH were measured using the Milliplex map kit (rat pituitary magnetic bead panel; Millipore).

Isolation of mitochondria from BAT

Mitochondria were isolated from BAT using a Percoll gradient as previously described (30), and the protein concentration was measured by the Folin-Lowry method using albumin as the standard (31).

Oxygen consumption

Oxygen consumption rates were measured by high-resolution respirometry (Oroboros Oxygraph-O2K) at 35°C. The assay medium contained 0.5 mM EGTA, 3 mM $MgCl_2$, 60 mM K-Mes, 20 mM taurine, 10 mM KH_2PO_4, 20 mM HEPES, 110 mM sucrose, 5 mM pyruvate plus malate, and 0.2 mM ADP. When indicated, 0.1% bovine serum albumin-fatty acid free (BSA-faf) and 3 mM GDP were added to inhibit UCP1.

ATP synthesis

ATP synthesis was determined measuring the incorporation of $^{32}P_i$ into [γ-32P] ATP. $^{32}P_i$ excess was extracted from the medium as phosphomolybdate with 2-butanol benzene, as previously described (30). The assay medium was the same as that used for the oxygen consumption measurement.

Heat generation

The heat generated by isolated BAT mitochondria was measured using an Omega isothermal titration calorimeter from Microcal, Inc. The calorimeter sample cell (1.5 mL) was filled with the reaction medium, and the reference cell was filled with Milli-Q water (Millipore). After equilibration at 35°C, the reaction was started by injecting mitochondria into the sample cell, and the heat change was recorded over a 20-minute period. Heat changes measured during the initial 2 minutes after the injection of mitochondria were discarded to avoid artifacts, such as changes resulting from the heat produced by the dilution of the mitochondria suspension (32).

Hepatic triglyceride and cholesterol content

Fifty milligrams of liver were homogenized with 350 μL of PBS and 350 μL of deoxycholic acid (0.25%) and incubated at 37°C for 5 minutes. Ten microliters of the homogenate were used to measure the hepatic triglyceride and cholesterol content using commercial kits (Bioclin).

RNA isolation and real-time PCR

Liver total RNA was extracted using the RNeasy Plus minikit (QIAGEN) in accordance with the manufacturer's instructions. After deoxyribonuclease treatment, reverse transcription was followed by real-time-PCR, which was performed as previously described (14, 33). Specific oligonucleotides, detailed in Supplemental Table 1, were purchased from Applied Biosystems. The peptidylprolyl isomerase A gene was used as an internal control for the rat liver.

Gel electrophoresis and immunoblotting

Liver tissue samples (50 mg) were homogenized in protein lysis buffer containing 150 mM NaCl, 1 mM $MgCl_2$, 2.7 mM KCl, 20 mM Tris (pH 8.0), 1% Triton X-100, 10% glycerol, 0.5 mM $NaVO_4$, 1 μM phenylmethylsulfonyl fluoride, 10 mM NaF, and both protease inhibitor and phosphatase inhibitor cocktails (Sigma P8340 and Sigma P0044, respectively) using a homogenizer (Ultra-Turrax T25; Fisher Scientific Inc). After centrifugation at 1500 $\times$ *g*, the supernatant was collected, and the protein concentration was determined using a bicinchoninic acid assay kit (Pierce) as instructed by the manufacturer. Protein samples were resolved on polyacrylamide SDS-PAGE gels according to Laemmli (34) as follows: 7.5% for AMP-activated protein kinase (AMPK) and acetyl-CoA carboxylase (ACC) proteins and 10% for phosphoenolpyruvate carboxykinase (PEPCK), glucose-6-phosphatase (G6Pase), and UCP1. Electrotransfer of proteins from the gel to polyvinylidene difluoride membranes was performed for 120 minutes at 110 V in a buffer consisting of 192 mM glycine and 20% methanol. The membranes were blocked with 5% BSA in Tris-buffered saline containing 0.1% Tween 20 for 1 hour at room temperature. The membranes were then incubated with primary antibodies (Supplemental Table 2) overnight at 4°C, after which they were washed and incubated with secondary antibody for 2 hours at room temperature. The detection of the immunocomplex was performed using an enhanced chemiluminescence detection kit.

Statistical analysis

Unless specified in the figure legend, data were analyzed by one-way ANOVA in each group of animals, at 12 or 21 days after OVX with respect to the correspondent SHAM and E2-treated rats, followed by the Newman-Keuls multiple-comparison test. Statistical analyses were performed using the software GraphPad Prism (version 5; GraphPad Software, Inc).

Results

Metabolic parameters

As previously reported (1, 35), we confirm that ovariectomy induced an increase in body weight gain at 12 and 21 days after the surgery, which was prevented by E2 treatment (Table 1 and Figure 1A). OVX rats had decreased uterine weight and serum E2 when compared with SHAM and OVX + E2 rats. These parameters were slightly greater in OVX + E2 compared with SHAM rats (Table 1). The efficacy of the surgery was also confirmed by higher serum FSH and LH levels in OVX rats (Table 1). In accordance with the well-known inhibitory effect of estradiol on appetite (7), OVX animals exhibited a significantly higher food intake than SHAM-operated and OVX + E2 rats (Figure 1B). To evaluate whether increased intestinal absorption could contribute to the increase in body weight gain, we also measured feces amount. In fact, OVX rats had a greater amount of feces at 21 days after ovariectomy (Figure 1C), which is most likely secondary to the increased food intake such that there was no difference in the ratio of feces/food intake between the three groups (Figure 1D). Food efficiency (body weight gain per food intake) was significantly greater in OVX compared with SHAM and OVX + E2 (Figure 1E), and these results show that at 12 days after ovariectomy, OVX rats are already prone to becoming overweight, which may be secondary to decreased energy expenditure.

Table 1. Metabolic Characteristics of SHAM, OVX and OVX + E2 at 12 and 21 Days After Surgery

	12 Days			21 Days		
	SHAM	OVX	OVX + E2	SHAM	OVX	OVX + E2
Body weight gain, g	26.3 ± 1.0[a]	43.4 ± 2.3[b]	26.4 ± 2.1[a]	36.9 ± 2.0[a]	64.4 ± 3.2[b]	31.8 ± 1.7[a]
E2, pg/mL	10.8 ± 2.96[a]	5.01 ± 0.01[b]	22.1 ± 1.98[c]	12.7 ± 1.99[a]	5.4 ± 0.50[b]	18.3 ± 4.42[a]
Progesterone	–	–	–	62.0 ± 26.5	5.8 ± 1.7	18.8 ± 4.2
FSH, ng/mL*	1.62	15.17	3.57	0.59	4.92	ND
FSH, minimum and maximum	(1.03–3.03)	(10.67–19.75)	(1.83–5.55)	(0.01–1.46)	(2.89–7.69)	ND
LH, ng/mL*	0.41	6.60	0.24	0.22	1.44	ND
LH, minimum and maximum	(0.27–0.58)	(2.41–18.99)	(0.11–0.48)	(0.09–0.27)	(0.84–2.1)	ND
Uterus weight, g	0.44 ± 0.05[a]	0.09 ± 0.01[b]	0.64 ± 0.06[c]	0.32 ± 0.02[a]	0.10 ± 0.02[b]	0.52 ± 0.03[c]
TG, mg/dL	46.3 ± 5.0[a]	46.8 ± 3.3[a]	68.3 ± 6.2[b]	45.5 ± 2.6	35.9 ± 2.4	47.1 ± 9.0
Total cholesterol, mg/dL	51.3 ± 2.7[a]	66.1 ± 2.1[b]	69.3 ± 3.4[b]	42.9 ± 3.1[a]	69.1 ± 5.1[b]	61.4 ± 5.3[b]
VLDL cholesterol, mg/dL	9.3 ± 1.0[a]	9.4 ± 0.7[a]	13.7 ± 1.3[b]	9.1 ± 0.5	7.2 ± 0.5	9.4 ± 1.8
LDL cholesterol, mg/dL	25.1 ± 1.7[a]	31.9 ± 1.3[b]	26.0 ± 2.3[a]	19.1 ± 2.6[a]	43.4 ± 7.4[b]	22.7 ± 1.1[a]
HDL cholesterol, mg/dL	21.8 ± 1.0[a]	24.8 ± 0.9[a]	30.2 ± 1.5[b]	11.7 ± 0.8[a]	16.3 ± 1.1[b]	23.8 ± 3.2[c]
Serum insulin, ng/dL	–	–	–	0.32 ± 0.1	0.27 ± 0.04	–

Abbreviation: ND, not detectable. Serum analysis was performed after an overnight fasting. Data are represented as average ± SEM of 6–18. Dashes mean not measured. Different letters mean averages were significantly different.

* FSH and LH are shown as median and range.

BAT thermogenic activity

It has been established that BAT morphology differs between male and female rats (15–17), but the effects of ovarian hormones on BAT mitochondria are still controversial (18, 36). To determine whether altered BAT thermogenesis could contribute to the increase in body weight gain observed after ovariectomy, we analyzed BAT thermogenic activity in OVX rats at 12 and 21 days after the surgery. There were no differences in BAT weight (Figure 2A). Although peroxisome proliferator-activated receptor γcoactivator 1-alpha (PGC-1α) was decreased after ovariectomy (Figure 2B), citrate synthase activity was not different between SHAM and OVX, which indicates that the mitochondrial content in BAT from short-term OVX animals was normal (Figure 2C). However, the ratio of BAT weight to body weight was already decreased in OVX rats compared with SHAM at 12 days after the surgery (SHAM 0.87 ± 0.05 vs OVX 0.76 ± 0.02, 12 d; SHAM 0.93 ± 0.03 vs OVX 0.79 ± 0.03, 21 d), probably due to increased body mass. Additionally, there were no differences

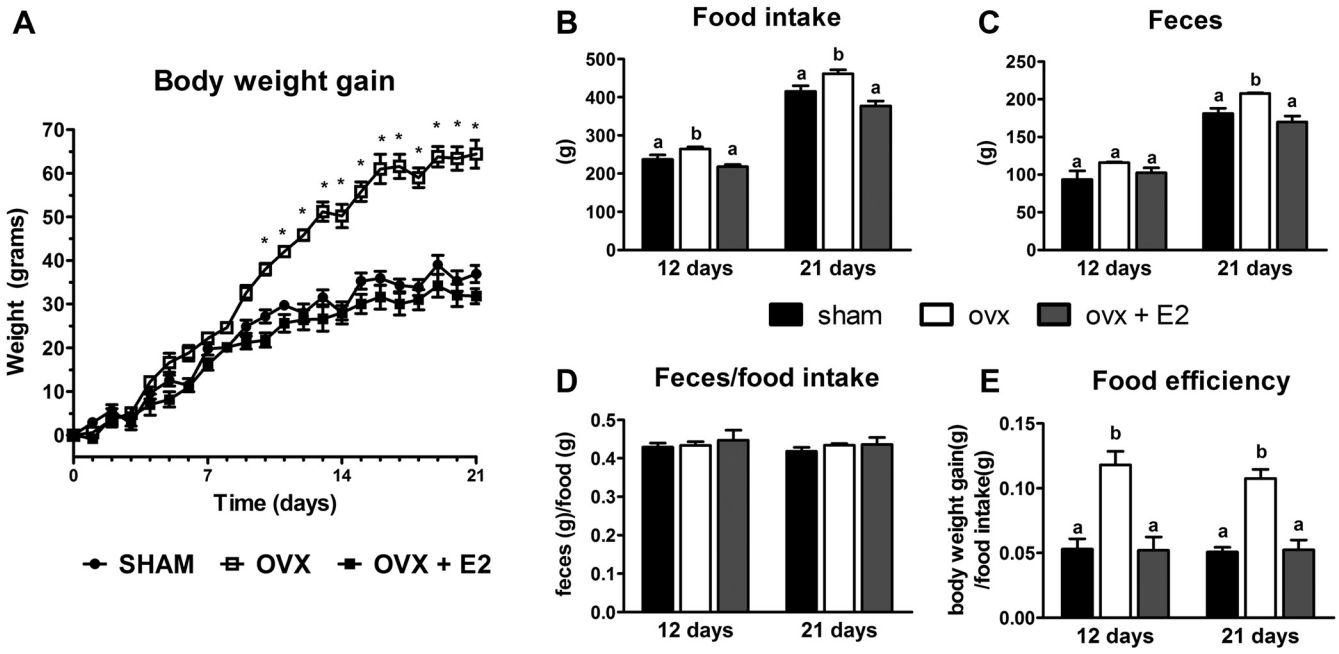

Figure 1. Effect of ovariectomy and E2 treatment on body weight gain, food intake, and feces amount. Body weight gain (A), food intake (B), and feces content (C) were measured throughout the 12 and 21 days after the surgery. Feces/food intake (D) and food efficiency (E) were calculated as grams of feces or b.w. gained per gram of food consumed. The figure represents average ± SEM of 4–19. Different letters mean averages were significantly different ($P < .05$) between the groups.

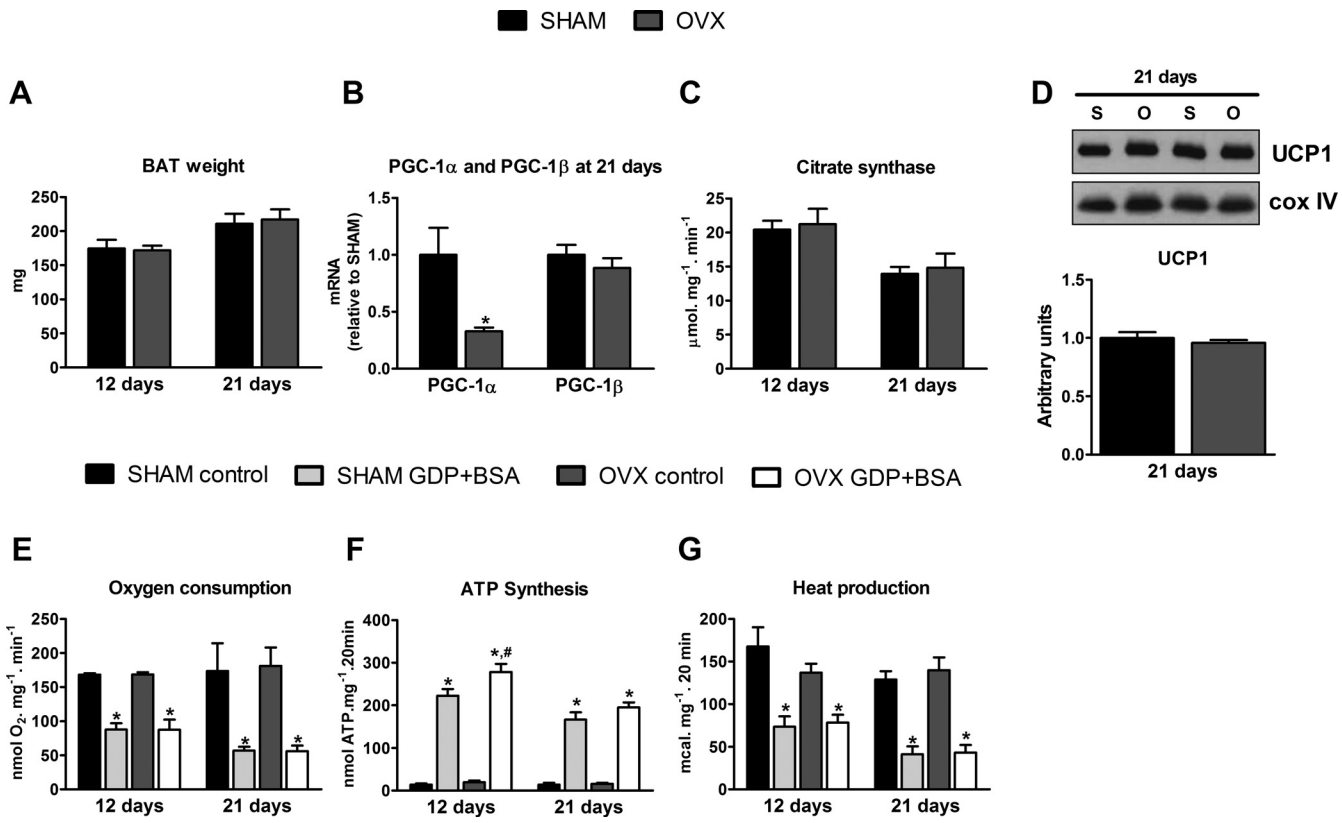

Figure 2. BAT thermogenic activity 12 and 21 days after ovariectomy. BAT was weighed (A); PGC-1α mRNA levels were relative to SHAM (B); citrate synthase activity was measured in total homogenate (C); mitochondria were isolated, and 2.5 μg was used to load the gel, and immunodetection was determined using UCP1 and CoxIV (subunit IV of complex IV, loading control) antibodies (representative). Densitometric analysis (average ± SE) represents arbitrary units relative to SHAM (D). Oxygen consumption (E) was measured in a high-resolution oxygraph (Oxygraph-2k; Oroboros). ATP synthesis (F) was measured radioactively. Heat production (G) was determined using an Omega isothermal titration calorimeter. Panels E, F, and G were measured in isolated mitochondria and the assay medium was as described under *Materials and Methods*. The figure represents average ± SEM of 4–10. *, $P < .05$ (vs control); #, $P < .05$ vs SHAM. O, OVX; S, SHAM.

in UCP1 expression in isolated BAT mitochondria from OVX rats at 21 days after the surgery (Figure 2D).

To evaluate mitochondrial physiology, we isolated mitochondria and measured their oxygen consumption, ATP synthesis, and heat production at 12 and 21 days after ovariectomy. When indicated, GDP and BSA were added to inhibit UCP1 activity. BAT mitochondrial oxygen consumption was not different between the SHAM and OVX rats; in both groups, oxygen consumption decreased in the presence of GDP and BSA (Figure 2E), as expected (37). A large increase in ATP synthesis was observed when UCP1 was inhibited in both groups, and the increment was slightly greater in the OVX rats compared with SHAM at 12 days after the surgery (Figure 2F). As expected, heat production followed the same pattern observed for oxygen consumption (Figure 2G). Altogether these results suggest that BAT mitochondria dysfunction is not implicated in the higher food efficiency found in short-term OVX animals.

Serum lipid profile

To determine whether changes in the lipid profile occur early after ovariectomy, even in animals eating a chow diet, we analyzed the serum lipid profile at 12 and 21 days after surgery. Serum fasting total cholesterol was greater in both OVX and OVX + E2 group at 12 and 21 days after ovariectomy. At 12 days, these higher levels were accounted for by increased LDL cholesterol in the OVX group and increased VLDL and HDL cholesterol in the OVX + E2 group (Table 1). This latter group also displayed higher levels of serum triglyceride. At 21 days, the increase in total cholesterol was accounted for by increased LDL and HDL cholesterol in the OVX group and increased HDL cholesterol in OVX + E2 rats. In contrast, OVX rats have slightly decreased serum triglyceride and VLDL cholesterol levels compared with SHAM and OVX + E2 (Table 1). We also measured mRNA levels for 3-hydroxy-3-methylglutaryl coenzyme A (HMG-CoA) reductase, an enzyme that plays an important role in cholesterol biosynthesis. Concomitant with the increase in total cholesterol, OVX and OVX + E2 rats displayed increased mRNA levels for HMG-CoA reductase at 21 days and at 12 and 21 days, respectively.

Hepatic lipid metabolism

Accumulation of fat in the liver was previously detected only 6 weeks after ovariectomy (38). We measured liver

triglyceride and cholesterol levels at 12 and 21 days after the surgery, ie, after a shorter period than previously described. Hepatic cholesterol was lower in OVX + E2 rats compared with SHAM and OVX at 12 days after ovariectomy and was increased in OVX rats compared with SHAM and OVX + E2 at 21 days after ovariectomy (Figure 3B). A similar result was observed for hepatic triglyceride content, although it did not reach statistical significance (Figure 3A). We measured mRNA levels for sterol regulatory element-binding protein 1c (SREBP1c), a transcription factor that targets important lipogenic genes. SREBP1c mRNA was slightly greater in both OVX and OVX + E2 compared with SHAM at 12 days after ovariectomy.

Phosphorylation of ACC by AMPK is one important step that regulates fatty acid synthesis and oxidation (3). We found that both ACC and AMPK were less phosphorylated in the liver of OVX rats compared with SHAM (Figure 3, D and E), which may explain the increased triglyceride content. E2 treatment partially prevented the decrease in pAMPK and pACC observed in OVX rats (Figure 3, D and E). Surprisingly, mRNA levels for AMPKα1 and AMPKα2 subunits were higher in OVX animals than in SHAM animals at 21 days after the surgery (Table 2). OVX and OVX + E2 rats displayed increased mRNA levels for AMPKβ1 compared with SHAM at 21 days and 12 and 21 days, respectively (Table 2). The level of liver kinase B1 (LKB1) mRNA, one of the kinases that phosphorylates AMPK, was also elevated in OVX and OVX + E2 compared with SHAM (Table 2), but LKB1 protein levels were not different between the groups (Figure 3C). Carnitine palmitoyltransferase 1a mRNA did not differ significantly in OVX and OVX + E2 compared with SHAM animals (Table 2). The increased mRNA levels of LKB1 and AMPK subunits in OVX and OVX + E2 compared with SHAM rats (Table 2) suggest that the liver transcriptional regulation of these genes are depend on ovarian mediators other than estrogen. However, pAMPK changes are directly related to estradiol effects because it has been shown that estradiol rapidly (minutes) increases pAMPK (3), and estrogen replacement was able to normalize liver pAMPK herein.

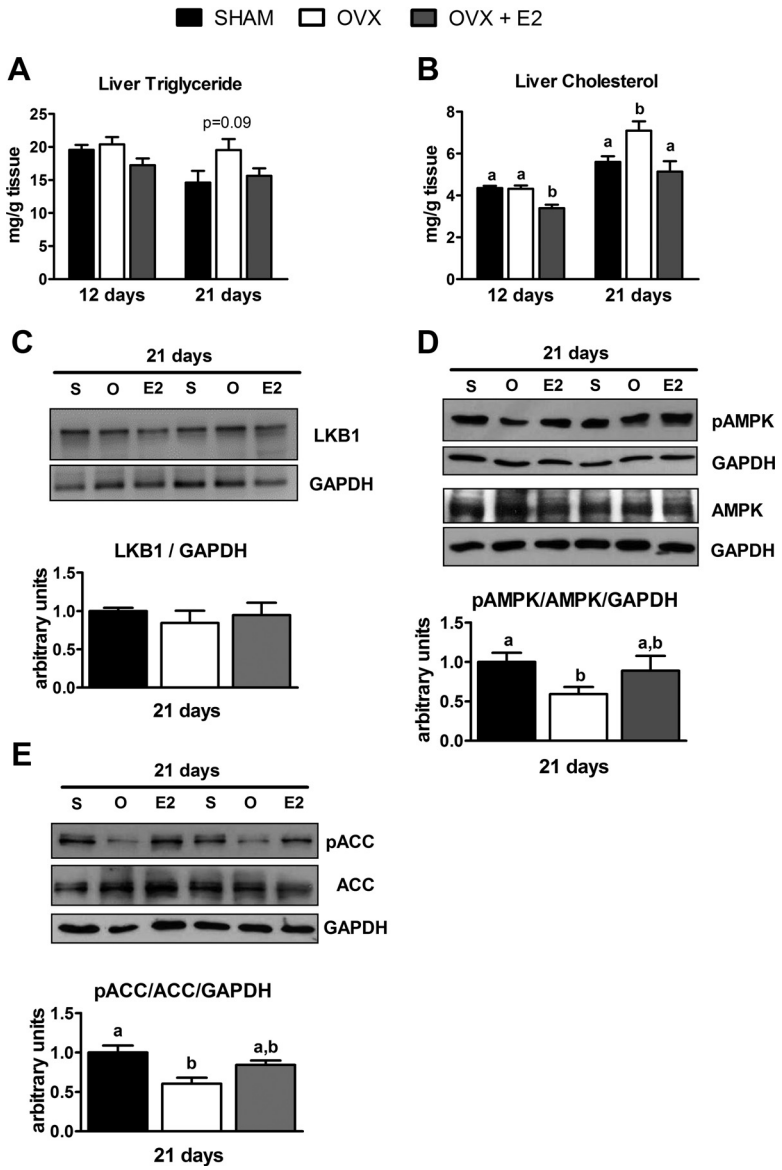

Figure 3. Effect of ovariectomy and E2 treatment on lipid metabolism in the liver. Liver TG (A) and cholesterol (B) were measured as described. Thirty micrograms of total homogenate were used to load the gel, and immunodetection was determined using LKB1 (C), pAMPK and AMPK (D), and pACC and ACC (E) antibodies (representative). Densitometric analysis represents arbitrary units relative to SHAM. The figure represents the average ± SEM of 4–15. Different letters mean averages were significantly different ($P < .05$) between the groups. GAPDH, glyceraldehyde-3-phosphate dehydrogenase; O, OVX; S, SHAM; E2, OVX treated with E2.

Insulin sensitivity and liver glucose metabolism

Despite their augmented body weight, after 21 days, the OVX rats had no impairment in the insulin (Figure 4A) and glucose tolerance tests (Figure 4B) and no changes in fasting serum insulin (Table 1). However, OVX rats had increased

Table 2. Real-Time PCR Analysis in Liver at 12 and 21 Days After Ovariectomy

	12 Days			21 Days		
Targets	**SHAM**	**OVX**	**OVX + E2**	**SHAM**	**OVX**	**OVX + E2**
Glycogen phosphorylase	1.00 ± 0.23	1.5 ± 0.22	1.53 ± 0.19	1.00 ± 0.10	1.53 ± 0.23	1.43 ± 0.23
LKB1	1.00 ± 0.17[a]	1.68 ± 0.24[b]	1.87 ± 0.21[b]	1.00 ± 0.07[a]	1.41 ± 0.01[b]	2.36 ± 0.27[c]
AMPKα1	1.00 ± 0.06	1.27 ± 0.19	1.16 ± 0.13	1.00 ± 0.03[a]	1.38 ± 0.12[b]	1.18 ± 0.15[a,b]
AMPKα2	1.00 ± 0.14	1.22 ± 0.09	1.20 ± 0.10	1.00 ± 0.05[a]	1.49 ± 0.17[b]	1.38 ± 0.15[a,b]
AMPKβ1	1.00 ± 0.10[a]	1.14 ± 0.12[a]	2.08 ± 0.13[b]	1.00 ± 0.07[a]	1.38 ± 0.12[b]	2.24 ± 0.28[c]
Glucagon receptor	1.00 ± 0.11[a]	1.49 ± 0.06[b]	1.32 ± 0.11[b]	1.00 ± 0.03[a]	1.32 ± 0.09[b]	0.97 ± 0.12[a]
PGC1α	1.00 ± 0.06	1.21 ± 0.29	1.22 ± 0.24	1.00 ± 0.08[a]	1.80 ± 0.30[b]	2.67 ± 0.42[c]
TRAF2	1.00 ± 0.06[a]	1.25 ± 0.16[a]	1.77 ± 0.19[b]	1.00 ± 0.06[a]	1.01 ± 0.07[a]	1.91 ± 0.17[b]
CPT1a	1.00 ± 0.15[a]	1.49 ± 0.21[b]	0.92 ± 0.08[a]	1.00 ± 0.04	1.42 ± 0.16	1.42 ± 0.13
CPT2	1.00 ± 0.07	1.41 ± 0.22	1.18 ± 0.11	1.00 ± 0.07	1.47 ± 0.27	1.22 ± 0.11
SREBP1c	1.00 ± 0.17	1.54 ± 0.19	1.78 ± 0.37	1.00 ± 0.07	1.66 ± 0.54	1.86 ± 0.38
HMG-CoA reductase	1.00 ± 0.17[a]	1.02 ± 0.17[a]	2.00 ± 0.32[b]	1.00 ± 0.20[a]	2.78 ± 0.53[b]	3.22 ± 0.53[b]

Abbreviation: CPT1a, carnitine palmitoyltransferase 1a. Data are represented as mean ± SEM of 5–11 animals. OVX and OVX + E2 data represent mRNA levels relative to SHAM. Different letters mean averages were significantly different.

glucose production during the pyruvate tolerance test when compared with SHAM at 21 days after ovariectomy (Figure 4C). Despite preventing body weight gain and hepatic triglyceride (TG) increase, E2 treatment did not prevent the increase in glucose production during the pyruvate tolerance test (Figure 4C). In fact, E2 treatment alone tended to increase glucose production at 12 days after ovariectomy (Figure 4C).

To gain further insight into the causes of the disrupted glucose metabolism usually observed after menopause, we measured the expression of enzymes that play an important role in hepatic glucose production. There was a significant increase in the mRNA levels of G6Pase in the liver of OVX animals when compared with SHAM and OVX + E2 rats. In fact, OVX + E2 rats had lower G6Pase mRNA levels than SHAM and OVX at 12 days after ovariectomy (Figure 5A). PEPCK mRNA levels were increased in OVX rats at 21 days after ovariectomy, and E2 treatment resulted in further increase (Figure 5C). G6Pase protein was also increased in OVX compared with SHAM and OVX + E2 rats at 21 days after ovariectomy (Figure 5B). PEPCK protein was increased in OVX + E2 compared with SHAM and OVX at 21 days after the surgery (Figure 5D). These results suggest that changes in enzymes that play important roles in gluconeogenesis could contribute to the increase in glucose production in OVX and OVX + E2 rats. The level of glycogen phosphorylase mRNA did not differ significantly in both OVX and OVX + E2 compared with SHAM (Table 2). The glucagon receptor mRNA level was elevated in OVX and OVX + E2 rats at 12 days after ovariectomy. E2 treatment restored glucagon receptor mRNA levels to that observed in the SHAM group at 21 days after the surgery (Table 2). These results suggest that an increased stimulation of the glucagon-signaling pathway could contribute to the increase in gluconeogenesis. Ovariectomy also promoted an increase in PGC-1α, a transcription factor that positively regulates PEPCK and G6Pase expression, at 21 days after ovariectomy (Table 2). E2 treatment further increased PGC-1α mRNA (Table 2). TNF receptor-associated factor 2 (TRAF2) is up-regulated in obese mice and is associated with increased gluconeogenesis and increased response to

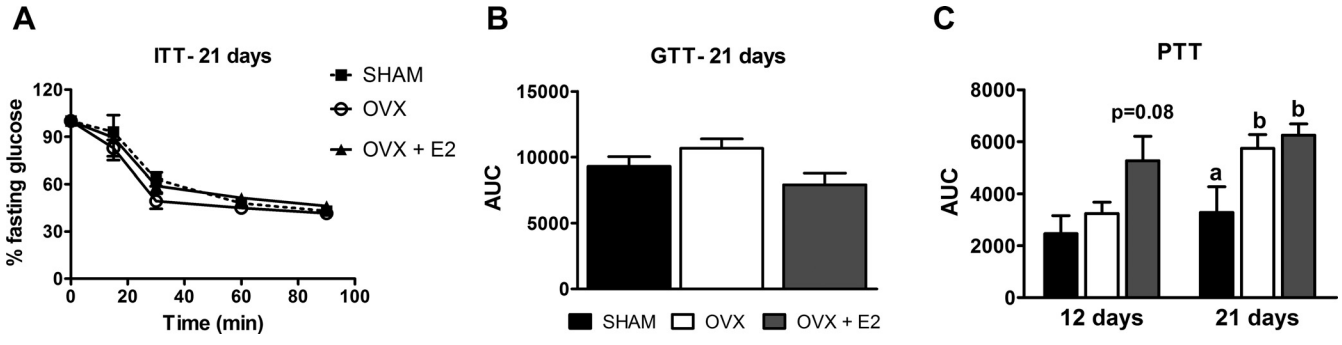

Figure 4. Effect of ovariectomy and E2 treatment on glucose metabolism. Insulin was injected ip and glucose concentration was measured (A). Glucose was injected ip and glucose concentration was measured (B); sodium pyruvate (2 g/kg) was injected ip and glucose concentration was measured (C). The figure represents the average ± SEM of 5–10. Different letters mean averages were significantly different ($P < .05$) between the groups. ITT, insulin tolerance test; GTT, glucose tolerance test; PTT, pyruvate tolerance test.

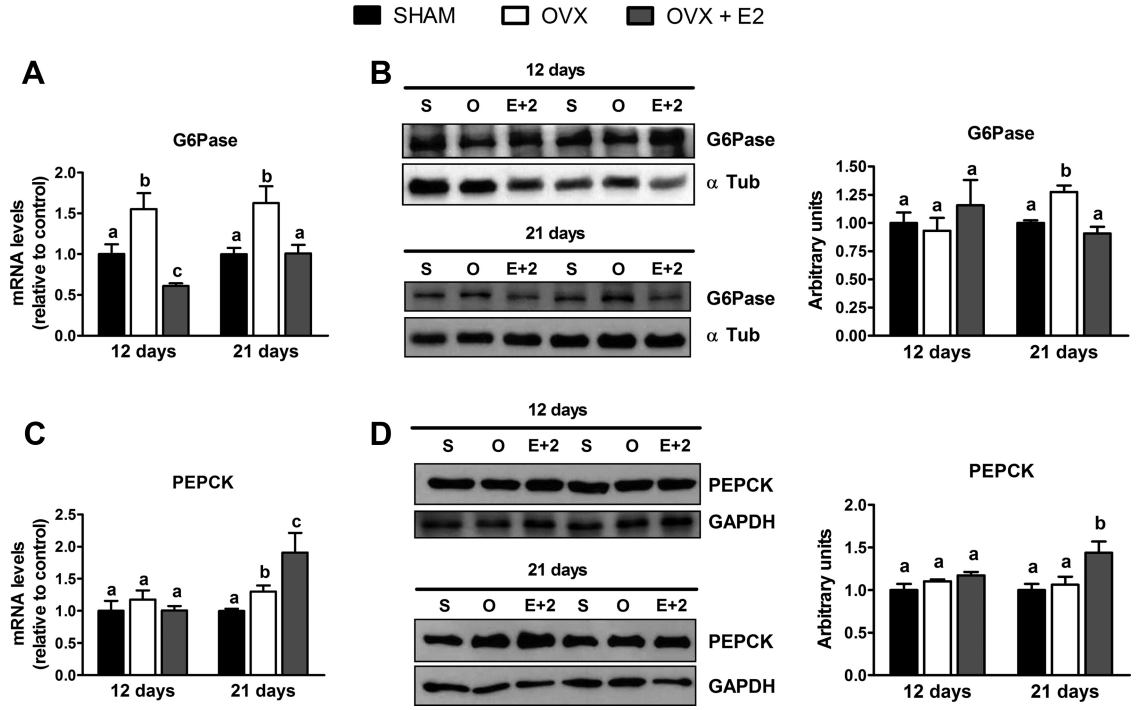

Figure 5. Effect of ovariectomy and E2 treatment on the expression of gluconeogenic enzymes. Quantitative real-time PCR (relative to the endogenous target gene *ppia*) was performed to determine the expression of G6Pase (A) and PEPCK (C). Thirty micrograms of total homogenate were used to load the gel, and immunodetection was determined using G6Pase, PEPCK, α-tubulin, and GAPDH antibodies. Densitometric analysis of G6Pase (B) and PEPCK (D) is shown. The figure represents the average ± SEM of 8–11. *, $P < .05$ (vs SHAM). Different letters mean averages were significantly different ($P < .05$) between the groups. GAPDH, glyceraldehyde-3-phosphate dehydrogenase; O, OVX; S, SHAM; TUB, tubulin.

glucagon (29); the TRAF2 mRNA level was elevated in OVX + E2 rats compared with SHAM and OVX at 12 and 21 days after the surgery (Table 2).

Discussion

The increase in body weight gain after ovariectomy is in accordance with previous studies describing the role of estradiol in the control of energy metabolism (1, 4, 7, 22). However, the metabolic changes that occur in the early phase of body weight gain due to estrogen deficiency have been poorly defined. We show that although food intake is slightly increased in OVX compared with SHAM and OVX + E2 rats, a corresponding increase occurs in the feces amount (Figure 1C), and no differences were detected in the feces to food intake ratio (Figure 1D). These new findings highlight that metabolic changes related to higher food efficiency are far more important for body weight gain than increased energy intake.

Studies in humans have shown a greater incidence of active BAT in women than in men (39, 40). To verify whether the increase in food efficiency (Figure 1E) could be due to decreased BAT oxygen consumption, we performed a detailed analysis of BAT mitochondria function at 12 and 21 days after ovariectomy. There were no differences in BAT weight, citrate synthase activity, and UCP1 protein content (Figure 2, A, C, and D) at 12 and 21 days after ovariectomy. Recently a small decrease in citrate synthase activity and an increase in UCP1 expression were reported in ovariectomized rats, but this experiment was performed 4 weeks after ovariectomy in animals that underwent the surgery at the age of 5 weeks (18). We have also shown that oxygen consumption was not different between SHAM and OVX, even in response to exercise (41). If altered BAT metabolism played a role in the early phase of body weight gain in ovariectomized rats, we should have observed a difference in mitochondrial parameters as soon as 12 or 21 days after ovariectomy. Oxygen consumption and heat production did not differ between SHAM and OVX animals at 12 and 21 days after ovariectomy (Figure 2, E and G). ATP synthesis was only slightly increased in OVX rats in the presence of GDP and BSA, suggesting that BAT mitochondria could be more coupled in the OVX group at 12 days after the surgery (Figure 2F). This increase in ATP synthesis, however, does not seem to alter BAT physiology because the major part of the electrochemical proton gradient is released as heat. These results show for the first time that differences in BAT metabolism do not contribute to the early phase of ovariectomy-induced weight gain.

Elevated levels of total cholesterol and HDL were reported in ArKO mice, a mouse model of estrogen deficiency (5). OVX rats had increased total cholesterol compared with SHAM at 12 days after the surgery, which persisted 21 days after ovariectomy. This increase was due to elevated LDL cholesterol at 12 days and increased HDL and LDL cholesterol at 21 days after the surgery. OVX + E2 rats also displayed increased total cholesterol compared with SHAM, but this change was due to elevated HDL cholesterol, which was also greater than the values observed in both SHAM and OVX rats (Table 1). The increased HMG-CoA reductase mRNA level in OVX and OVX + E2 compared with SHAM rats (Table 2) suggests increased cholesterol biosynthesis could be contributing to the increase in serum cholesterol. However, we cannot assure that HMG-CoA reductase activity is increased in both OVX and OVX + E2 because its activity is also regulated by other factors such as phosphorylation by AMPK (42). In fact, Trapani et al (43) suggested that the increased HMG-CoA reductase in aged females compared with 3-month-old females was associated with decreased AMPK phosphorylation in aged females.

We also observed a decrease in pAMPK in the liver of OVX when compared with SHAM rats (Figure 3D), which was prevented by estrogen replacement. In agreement, OVX + E2 rats displayed lower hepatic cholesterol content than SHAM and OVX rats (Figure 3B). On the other hand, increased serum TG levels in OVX + E2 rats at 12 days after ovariectomy (Table 1) could be explained by greater VLDL synthesis or secretion (44). Zhu et al (22) reported increased TG export from the liver in OVX + E2 compared with OVX mice that received a high-fat diet for 5 weeks. They suggest this result contributes to the decrease in hepatic TG content after E2 treatment (22).

This seems to be the case in our experiments because hepatic TG tended to be increased (Figure 3A), and serum TG (Table 1) was decreased in OVX compared with SHAM and OVX + E2 rats at 21 days after the surgery. The increase in liver TG was accompanied by a reduction in pAMPK and pACC in OVX compared with SHAM rats (Figure 3, D and E). Because AMPK activation suppresses ACC activity, lower levels of pAMPK and pACC can lead to decreased fatty acid oxidation and lipogenesis stimulation. In support of our findings, decreased palmitate oxidation was observed in liver slices of OVX Sprague Dawley rats at 5 weeks after ovariectomy (45). Moreover, isolated hepatocytes from OVX mice displayed lower oxygen consumption than OVX receiving E2 when palmitate was used as the substrate (10). Also consistent with our data, Kim et al (27) reported decreased pAMPK and pACC levels not only in liver but also in skeletal muscle and adipose tissue in mice at 2 and 10 weeks after ovariectomy. We also measured mRNA level of SREBP1c, a transcription factor that targets important lipogenic genes, and we found it was elevated in OVX and OVX + E2 compared with SHAM rats at 12 days after ovariectomy (Table 2). However, we cannot affirm this change results in increased activity of this transcription factors since SREBP1 is synthesized as a precursor protein bound to the membranes of the endoplasmic reticulum and must be liberated by a cleavage process (46).

Surprisingly, we observed increased liver mRNA levels of AMPK subunits and LKB1 after ovariectomy (Table 2), which are not prevented by estradiol treatment. LKB1 protein levels were not changed though (Figure 3C). The ovarian hormones effect on LKB1 expression is interesting and further studies are necessary to fully understand how LKB1 expression is regulated after ovariectomy and estradiol treatment. However, it was recently shown that ERα binds to the LKB1 promoter in a ligand-independent manner and enhances its expression in human breast cancer cells (47) and that the balance between androgens and estrogens can regulate LKB1 expression in white adipocytes (48). The changes in pAMPK levels, however, could be a direct and rapid effect of estradiol, as previously reported in myocytes (3).

OVX mice display increased PEPCK and G6Pase mRNA levels 2 weeks after ovariectomy (27). We show that not only the mRNA but also G6Pase protein levels are increased in OVX compared with SHAM and OVX + E2 rats (Figure 5, A and B, respectively). Moreover, OVX + E2 rats had decreased G6Pase mRNA levels compared with SHAM and OVX rats at 12 days after ovariectomy (Figure 5A), which was already reported by Bryzgalova et al (23). The changes in G6Pase mRNA levels cannot be explained by differences in PGC-1α mRNA level because it was not changed at 12 days after ovariectomy, and the highest level was found in OVX + E2 rats at 21 days after the surgery (Table 2). The discrepancy between PGC-1α and G6Pase expression can be associated with differences in PGC-1α activity, which is also regulated by acetylation (49). Surprisingly, PEPCK mRNA and protein levels were increased in OVX + E2 compared with SHAM and OVX rats at 21 days after ovariectomy (Figure 5, C and D, respectively). Concomitant with increased G6Pase and PEPCK expression in OVX and OVX+ E2, respectively, both groups produced more glucose during the pyruvate tolerance test at 21 days after the surgery (Figure 4C), suggesting changes in gluconeogenic enzymes plays a pivotal role in this process. In addition, the elevated levels of gluconeogenic enzymes were coincident with the up-regulation of glucagon receptor mRNA in OVX and OVX + E2 rats at 12 days after ovariectomy (Table 2). Moreover, the increase in glucose production in OVX + E2 rats can

also be associated with increased TRAF2 expression (Table 2) because this factor was recently associated with an increase response to glucagon. Additionally, we could not detect any alterations in glucose and insulin tolerance tests and in serum insulin (Figure 4, A and B, and Table 1). In fact, we observed that even at 7 weeks after ovariectomy, the insulin tolerance test was not yet altered (data not shown). We thus speculate that the insulin resistance that occurs in estrogen-deficient animals is a consequence rather than the cause of obesity.

Postmenopausal women receiving E2 have decreased hepatic glucose production and glucagon levels in response to hypoglycemia when compared with women not receiving E2 (50). However, Liu et al (28) showed that E2 injection in the ventromedial hypothalamus of OVX rats that were not yet obese actually increased endogenous glucose production. Moreover, increased glucagon receptor expression in the liver is usually associated with a greater response to glucagon (51). These results suggest that increased glucagon signaling may partially account for the changes in the gluconeogenic enzymes in OVX and OVX + E2 rats, but further experiments are necessary to confirm these data. The increase in gluconeogenesis observed in OVX rats are not related to decreased E2 signaling in the hypothalamus because E2 replacement did not prevent the increase in glucose production during the pyruvate tolerance test (Figure 4C). The hypothalamus plays a key role in the regulation of glucose production. Musatov et al (8) reported an increased food intake in response to a 2-deoxy-D-glucose injection in the ventromedial nucleus of the hypothalamus in ERα knockout mice. Moreover, estradiol administration to OVX mice decreases the hypothalamic response to hypoglycemia (52), and OVX mice fed a high-fat diet and treated with intracerebroventricular E2 display decreased liver mRNA levels of PEPCK and G6Pase compared with OVX mice that do not receive estradiol (53). The results of Liu et al (28), however, show that E2 in the ventromedial nucleus of the hypothalamus actually increases endogenous glucose production before the onset of obesity. Thus, more experiments are necessary to understand whether the increase in glucose production in OVX + E2 rats observed in our experiments are caused by E2 effect on the hypothalamus.

In summary, our results show that ovariectomy leads to increased food efficiency, which cannot be explained by decreased BAT activity or increased intestinal absorption. Moreover, although estradiol treatment prevented the increase in body weight gain and hepatic TG and cholesterol accumulation induced by ovariectomy, it was not able to prevent increased gluconeogenesis. These results suggest disrupted liver glucose homeostasis after ovariectomy is caused by neither estradiol deficiency nor increased body weight or hepatic steatosis. Moreover, estrogen deficiency is directly related to the early-onset changes in liver cholesterol and triacylglycerol synthesis that precede the obese phenotype.

Acknowledgments

This article is dedicated to the memory of Professor Ricardo Renzo Bretani.

Address all correspondence and requests for reprints to: Leopoldo de Meis, MD, Instituto de Bioquímica Médica, CCS-Bloco E-Cidade Universitária, Ilha do Fundão, Rio de Janeiro, 21941–902, Brasil. E-mail: demeis@bioqmed.ufrj.br.

This work was supported by grants from the Fundação Carlos Chagas Filho de Amparo à Pesquisa do Estado do Rio de Janeiro (Programa de Apoio a Núcleos de Excelência) and the Conselho Nacional de Desenvolvimento Científico e Tecnológico. M.N., A.T.S., and R.A.N.L. were recipients of fellowships from Conselho Nacional de Desenvolvimento Científico e Tecnológico, and C.S.B. was the recipient of a fellowship from the Fundação Carlos Chagas Filho de Amparo à Pesquisa do Estado do Rio de Janeiro.

Disclosure Summary: The authors report no potential conflicts of interest relevant to this article.

References

1. **Rogers NH, Perfield JW 2nd, Strissel KJ, Obin MS, Greenberg AS.** Reduced energy expenditure and increased inflammation are early events in the development of ovariectomy-induced obesity. *Endocrinology*. 2009;150:2161–2168.
2. **Barros RP, Gustafsson JA.** Estrogen receptors and the metabolic network. *Cell Metab*. 2011;14:289–299.
3. **D'Eon TM, Souza SC, Aronovitz M, Obin MS, Fried SK, Greenberg AS.** Estrogen regulation of adiposity and fuel partitioning. Evidence of genomic and non-genomic regulation of lipogenic and oxidative pathways. *J Biol Chem*. 2005;280:35983–35991.
4. **Vieira Potter VJ, Strissel KJ, Xie C, et al.** Adipose tissue inflammation and reduced insulin sensitivity in ovariectomized mice occurs in the absence of increased adiposity. *Endocrinology*. 2012;153:4266–4277.
5. **Jones ME, Thorburn AW, Britt KL, et al.** Aromatase-deficient (ArKO) mice have a phenotype of increased adiposity. *Proc Natl Acad Sci USA*. 2000;97:12735–12740.
6. **Heine PA, Taylor JA, Iwamoto GA, Lubahn DB, Cooke PS.** Increased adipose tissue in male and female estrogen receptor-alpha knockout mice. *Proc Natl Acad Sci USA*. 2000;97:12729–12734.
7. **Gao Q, Mezei G, Nie Y, et al.** Anorectic estrogen mimics leptin's effect on the rewiring of melanocortin cells and Stat3 signaling in obese animals. *Nat Med*. 2007;13:89–94.
8. **Musatov S, Chen W, Pfaff DW, et al.** Silencing of estrogen receptor α in the ventromedial nucleus of hypothalamus leads to metabolic syndrome. *Proc Natl Acad Sci USA*. 2007;104:2501–2506.
9. **Xu Y, Nedungadi TP, Zhu L, et al.** Distinct hypothalamic neurons mediate estrogenic effects on energy homeostasis and reproduction. *Cell Metab*. 2011;14:453–465.
10. **Camporez JP, Jornayvaz FR, Lee HY, et al.** Cellular mechanism by which estradiol protects female ovariectomized mice from high-fat diet-induced hepatic and muscle insulin resistance. *Endocrinology*. 2013;154(3):1021–1028.

11. **Tseng YH, Cypess AM, Kahn CR.** Cellular bioenergetics as a target for obesity therapy. *Nat Rev Drug Discov*. 2010;9:465–482.
12. **Pedersen SB, Bruun JM, Kristensen K, Richelsen B.** Regulation of UCP1, UCP2, and UCP3 mRNA expression in brown adipose tissue, white adipose tissue, and skeletal muscle in rats by estrogen. *Biochem Biophys Res Commun*. 2001;288:191–197.
13. **Richard D, Picard F.** Brown fat biology and thermogenesis. *Front Biosci*. 2011;16:1233–1260.
14. **Wu J, Bostrom P, Sparks LM, et al.** Beige adipocytes are a distinct type of thermogenic fat cell in mouse and human. *Cell*. 2012;150:366–376.
15. **Quevedo S, Roca P, Pico C, Palou A.** Sex-associated differences in cold-induced UCP1 synthesis in rodent brown adipose tissue. *Pflugers Arch*. 1998;436:689–695.
16. **Rodriguez E, Monjo M, Rodriguez-Cuenca S, et al.** Sexual dimorphism in the adrenergic control of rat brown adipose tissue response to overfeeding. *Pflugers Arch*. 2001;442:396–403.
17. **Rodriguez-Cuenca S, Pujol E, Justo R, et al.** Sex-dependent thermogenesis, differences in mitochondrial morphology and function, and adrenergic response in brown adipose tissue. *J Biol Chem*. 2002;277:42958–42963.
18. **Nadal-Casellas A, Proenza AM, Llado I, Gianotti M.** Effects of ovariectomy and 17-β estradiol replacement on rat brown adipose tissue mitochondrial function. *Steroids*. 2011;76:1051–1056.
19. **Volzke H, Schwarz S, Baumeister SE, et al.** Menopausal status and hepatic steatosis in a general female population. *Gut*. 2007;56:594–595.
20. **Mauvais-Jarvis F, Clegg DJ, Hevener AL.** The role of estrogens in control of energy balance and glucose homeostasis. *Endocr Rev*. 2013;34(3):309–338.
21. **Gao J, He J, Shi X, et al.** Sex-specific effect of estrogen sulfotransferase on mouse models of type 2 diabetes. *Diabetes*. 2012;61:1543–1551.
22. **Zhu L, Brown WC, Cai Q, et al.** Estrogen treatment after ovariectomy protects against fatty liver and may improve pathway-selective insulin resistance. *Diabetes*. 2013;62(2):424–434.
23. **Bryzgalova G, Lundholm L, Portwood N, et al.** Mechanisms of antidiabetogenic and body weight-lowering effects of estrogen in high-fat diet-fed mice. *Am J Physiol Endocrinol Metab*. 2008;295:E904–E912.
24. **Nemoto Y, Toda K, Fujikawa-Adachi K, et al.** Altered expression of fatty acid-metabolizing enzymes in aromatase-deficient mice. *J Clin Invest*. 2000;105:1819–1825.
25. **Ahmed-Sorour H, Bailey CJ.** Role of ovarian hormones in the long-term control of glucose homeostasis, glycogen formation and gluconeogenesis. *Ann Nutr Metab*. 1981;25:208–212.
26. **Bryzgalova G, Gao H, Ahren B, et al.** Evidence that oestrogen receptor-α plays an important role in the regulation of glucose homeostasis in mice: insulin sensitivity in the liver. *Diabetologia*. 2006;49:588–597.
27. **Kim JY, Jo KJ, Kim OS, et al.** Parenteral 17β-estradiol decreases fasting blood glucose levels in non-obese mice with short-term ovariectomy. *Life Sci*. 2010;87:358–366.
28. **Liu J, Bisschop PH, Eggels L, et al.** Intrahypothalamic estradiol regulates glucose metabolism via the sympathetic nervous system in female rats. *Diabetes*. 2013;62:435–443.
29. **Chen Z, Sheng L, Shen H, et al.** Hepatic TRAF2 regulates glucose metabolism through enhancing glucagon responses. *Diabetes*. 2012;61:566–573.
30. **de Meis L, Ketzer LA, da Costa RM, de Andrade IR, Benchimol M.** Fusion of the endoplasmic reticulum and mitochondrial outer membrane in rats brown adipose tissue: activation of thermogenesis by Ca2+. *PLoS One*. 2010;5:e9439.
31. **Stauffer CE.** A linear standard curve for the Folin Lowry determination of protein. *Anal Biochem*. 1975;69:646–648.
32. **De Meis L, Ketzer LA, Camacho-Pereira J, Galina A.** Brown adipose tissue mitochondria: modulation by GDP and fatty acids depends on the respiratory substrates. *Biosci Rep*. 2012;32:53–59.
33. **Schmittgen TD, Lee EJ, Jiang J, et al.** Real-time PCR quantification of precursor and mature microRNA. *Methods*. 2008;44:31–38.
34. **Laemmli UK.** Cleavage of structural proteins during the assembly of the head of bacteriophage T4. *Nature*. 1970;227:680–685.
35. **Roesch DM.** Effects of selective estrogen receptor agonists on food intake and body weight gain in rats. *Physiol Behav*. 2006;87:39–44.
36. **Quarta C, Mazza R, Pasquali R, Pagotto U.** Role of sex hormones in modulation of brown adipose tissue activity. *J Mol Endocrinol*. 2012;49:R1–R7.
37. **Shabalina IG, Ost M, Petrovic N, Vrbacky M, Nedergaard J, Cannon B.** Uncoupling protein-1 is not leaky. *Biochim Biophys Acta*. 2010;1797:773–784.
38. **Pighon A, Gutkowska J, Jankowski M, Rabasa-Lhoret R, Lavoie JM.** Exercise training in ovariectomized rats stimulates estrogenic-like effects on expression of genes involved in lipid accumulation and subclinical inflammation in liver. *Metabolism*. 2011;60:629–639.
39. **Cypess AM, Lehman S, Williams G, et al.** Identification and importance of brown adipose tissue in adult humans. *N Engl J Med*. 2009;360:1509–1517.
40. **Pfannenberg C, Werner MK, Ripkens S, et al.** Impact of age on the relationships of brown adipose tissue with sex and adiposity in humans. *Diabetes*. 2010;59:1789–1793.
41. **Ignacio DL, Fortunato RS, Neto RA, et al.** Blunted response of pituitary type 1 and brown adipose tissue type 2 deiodinases to swimming training in ovariectomized rats. *Horm Metab Res*. 2012;44:797–803.
42. **Steinberg GR, Kemp BE.** AMPK in health and disease. *Physiol Rev*. 2009;89:1025–1078.
43. **Trapani L, Violo F, Pallottini V.** Hypercholesterolemia and 3-hydroxy-3-methylglutaryl coenzyme A reductase regulation in aged female rats. *Exp Gerontol*. 2010;45:119–128.
44. **Barsalani R, Chapados NA, Lavoie JM.** Hepatic VLDL-TG production and MTP gene expression are decreased in ovariectomized rats: effects of exercise training. *Horm Metab Res*. 2010;42:860–867.
45. **Paquette A, Chapados NA, Bergeron R, Lavoie JM.** Fatty acid oxidation is decreased in the liver of ovariectomized rats. *Horm Metab Res*. 2009;41:511–515.
46. **Ferre P, Foufelle F.** Hepatic steatosis: a role for de novo lipogenesis and the transcription factor SREBP-1c. *Diabetes Obes Metab*. 2010;12(suppl 2):83–92.
47. **Tulipano G, Faggi L, Cacciamali A, Spinello M, Cocchi D, Giustina A.** Interplay between the intracellular energy sensor AMP-activated protein kinase (AMPK) and the estrogen receptor activities in regulating rat pituitary tumor cell (GH3) growth in vitro. *Pituitary*. 2014;17(3):203–209.
48. **McInnes KJ, Brown KA, Hunger NI, Simpson ER.** Regulation of LKB1 expression by sex hormones in adipocytes. *Int J Obes (Lond)*. 2012;36:982–985.
49. **Lin HV, Accili D.** Hormonal regulation of hepatic glucose production in health and disease. *Cell Metab*. 2011;14:9–19.
50. **Sandoval DA, Ertl AC, Richardson MA, Tate DB, Davis SN.** Estrogen blunts neuroendocrine and metabolic responses to hypoglycemia. *Diabetes*. 2003;52:1749–1755.
51. **Lizarraga-Mollinedo E, Fernandez-Millan E, Martin Jde T, Martinez-Honduvilla C, Escriva F, Alvarez C.** Early undernutrition induces glucagon resistance and insulin hypersensitivity in the liver of suckling rats. *Am J Physiol Endocrinol Metab*. 2012;302:E1070–E1077.
52. **Cheng H, Isoda F, Mobbs CV.** Estradiol impairs hypothalamic molecular responses to hypoglycemia. *Brain Res*. 2009;1280:77–83.
53. **Yonezawa R, Wada T, Matsumoto N, et al.** Central versus peripheral impact of estradiol on the impaired glucose metabolism in ovariectomized mice on a high-fat diet. *Am J Physiol Endocrinol Metab*. 2012;303:E445–E456.